Archives of Materials Science and Engineering

Volume 112
Issue 1
November 2021
Pages 5-12

International Scientific Journal
published monthly by the
World Academy of Materials
and Manufacturing Engineering

DOI: 10.5604/01.3001.0015.5927

Structure and electrochemical behaviour of weldments of titanium Grade 1 in a bromine-containing solution

M.D. Ilieva *, N.V. Ferdinandov, D.D. Gospodinov, R.H. Radev
Department of Materials Science and Technology, "Angel Kanchev" University of Ruse,
8 Studentska str., POB 7017, Ruse, Bulgaria
* Corresponding e-mail address: mdilieva@uni-ruse.bg
ORCID identifier: https://orcid.org/0000-0001-7962-0760 (M.D.I.)

ABSTRACT

Purpose: The presented research aims to determine the microstructural changes in weldments of commercially pure titanium Grade 1 after welding by hollow cathode arc discharge in vacuum and related changes in the corrosion behaviour of the weldments.

Design/methodology/approach: Macro and microstructure of weldments were studied using optical microscopy. Corrosion behaviour of untreated Grade 1 and heat-affected zone of weldments of Grade 1 was investigated using electrochemical testing, including open circuit potential measurements and potentiodynamic polarisation. As an aggressive environment, 1 M KBr water solution was used.

Findings: Welding by hollow cathode arc discharge in vacuum leads to the formation of a coarse Widmanstätten structure in the heat-affected zone. This imperfect structure results in a passive layer with worsened protective properties, thus increasing the corrosion rate of weldments by up to two orders of magnitude compared to Grade 1 in as-received condition. The passive layer on the welded surfaces did not allow Grade 1 to acquire a stable corrosion potential during potenitodynamic polarization.

Research limitations/implications: Titanium and its alloys are passivating metallic materials, and their corrosion resistance depends on the properties of a thin protective surface layer. Changes in the underlying metal microstructure can affect the passivation behaviour of titanium and the properties of this layer. Welding by hollow cathode arc discharge in vacuum alters the microstructure of heat-affected zone, thereby causing Widmanstätten microstructure to form. As the passive layer over that microstructure has worsened protective properties, we suggest additional heat treatment after welding to be applied. Future experimental research on this topic is needed.

Originality/value: Welding by hollow cathode arc discharge in vacuum is a welding method allowing weldments to be done in a clean environment and even in space. In the specialised literature, information on the structure and corrosion resistance of weldments of commercially pure titanium Grade 1 welded by hollow cathode arc discharge in vacuum is missing. The present research fills in a tiny part of this gap in our knowledge.

Keywords: Titanium Grade 1, Hollow cathode arc discharge welding, Electrochemical corrosion, Cathodic loop

Reference to this paper should be given in the following way:
M.D. Ilieva, N.V. Ferdinandov, D.D. Gospodinov, R.H. Radev, Structure and electrochemical behaviour of weldments of titanium Grade 1 in a bromine-containing solution, Archives of Materials Science and Engineering 112/1 (2021) 5-12.
DOI: https://doi.org/10.5604/01.3001.0015.5927

MATERIALS

1. Introduction

Since titanium-based alloys possess good mechanical properties and a low density to strength ratio, they are the preferred material in aerospace and spacecraft industries. Furthermore, titanium and its alloys are used as a biocompatible material [1,2], and as a material for reinforced aluminium alloys matrix composite [3]. Most constructions of titanium alloys are usually joined using welding process. As titanium has a high affinity to oxygen and hydrogen, one of the shortcomings of titanium alloys during welding is the possibility for interaction with these two elements, leading to brittleness. This can be avoided using protective atmospheres such as inert gas or vacuum. Thus, welding by hollow cathode arc discharge in vacuum allows producing free of impurities weldments. Since titanium and its alloys are used in the aerospace industry, hollow cathode arc discharge in vacuum offers a good possibility for welding in space as shown in [4,5].

It is a well-known fact that titanium possesses excellent corrosion resistance. Despite being a highly reactive metal, titanium is a passivating metal as described in [6], i.e. when titanium is exposed to air or to an environment containing moisture, a thin protective surface oxide film of TiO_2 forms spontaneously [6-8]. The strong affinity of titanium for oxygen leads to an instant repair of this oxide film in the presence of even small quantities of oxygen or moisture [7]. Thus, the corrosion behaviour of titanium and its alloys depends on the stability and properties of the protective surface oxide film. Nevertheless, as corrosion resistance depends not only on the material properties but on the characteristics of the environment too, a material with absolute corrosion resistance does not exist. All metals, including titanium and its alloys, are prone to corrosion damage in specific media at specific conditions. The specialised literature reveals that titanium and its alloys suffer pitting corrosion in bromine solutions. Beck [9,10] has described the mechanism of pitting corrosion on titanium surface in bromine-containing media. Experiments in similar media were also done by other researchers [11-15].

In our previous work [16], we have shown severe pitting corrosion of weldments of titanium Grade 5 in a bromine-containing solution. Thus, as titanium and its alloys are corrosion resistant in the most used media, bromine solutions are suitable to estimate titanium corrosion properties and the influence of different technological processes on those properties. Unfortunately, data on the corrosion behaviour of weldments of titanium alloys produced using hollow cathode arc discharge in vacuum are missing in the specialised literature.

The present work aims to assess the influence of hollow cathode arc discharge welding in vacuum on the structure and corrosion properties of CP titanium alloy Grade 1.

2. Materials and methodology

2.1. Materials

The objects of the present study were weldments of commercially pure titanium CP-Ti Grade 1 with nominal chemical composition in weigth per cent as shown in Table 1. Using Niton™ XL2 handheld XRF Analyser, the iron content in the studied here CP-Ti was found to be 0.117 wt%. Welding was done by hollow cathode arc discharge in vacuum using the welding modes shown in Table 2. The welded sheets were with dimensions 100 x 50 x 2 mm. More information about the welding process can be found in [17].

Table 1.
Chemical composition of CP-Ti Grade 1

The maximum content of elements in CP-Ti Grade 1, wt%				
Fe	O	N	C	H
0.20	0.18	0.03	0.1	0.015

Table 2.
Welding modes

Welding mode No	Current, A	Welding speed, mm s^{-1}	Cathode shape and size	Plasma-forming gas flow rate, l h^{-1}
1	115	4.2	Round, Ø 4 mm	2.3-2.4
4	130	6.5	Elliptycal, 5.6x2	2.3-.4

The electrochemically tested specimens were made after tensile testing of the weldments, done previously on Instron 3384 machine [17]. Figure 1 represents the fractured weldments; parts of them at the fracture spot were cut and used for corrosion assessment of the weldments. It is visible from Figure 1 that the fracture occurred at the heat-affected zone, i.e., electrochemical testing was performed on the heat-affected zone. The tested specimens were designated as follows: Delivery for the untreated CP-Ti Grade 1, S1 for the specimen welded according to mode 1, and S4 for the specimen welded according to mode 4.

2.2. Testing methods

The macrostructure of the weldments was revealed after grinding, using a reagent containing 15 ml of HNO_3, 10 ml of HF and 75 ml of dH_2O, and was observed using microscope inspection tool. The microstructure was studied by optical microscopy after grinding, polishing and etching with a mixture of 30 ml of $C_3H_6O_3$, 10 ml of HF, and 10 ml of HNO_3. The grain size was determined using ImageJ software [18].

Fig. 1. Weldments after tensile testing: a) specimen S1; b) specimen S4

Before electrochemical tests, grinding and polishing were applied to the specimens; then the specimens were washed and degreased. Electrochemical testing was carried out at room temperature in a 1 M KBr water solution open to air. Two tests were performed: 1) measurement of open circuit potential for 60 minutes; 2) potentiodynamic polarisation in the range of -450 mV (NHE) to +1400 mV (NHE) using a RADELKIS OH-405 potentiostat connected to a USB digital controller NI-USB 6008 and a computer. A standard three-electrode cell, consisting of a saturated calomel electrode as reference electrode, a Pt counter electrode and the studied specimen as a working electrode, was used. The working electrode area was 0.19 cm^2. All presented here potentials were calculated against the normal hydrogen electrode. To determine the electrochemical characteristics of the specimens by Tafel analysis eL-Chem viewer software was used [19].

Corrosion rates were calculated from the determined from Tafel analysis corrosion current densities according to ASTM G 102-89 [20,21], using the following equation:

$$CR = K_1 \frac{i_{cor}}{\rho} EW \quad (1)$$

where:

- CR is the corrosion rate in mm y^{-1};
- $K_1 = 3.27 \cdot 10^{-3}$, mm g μA^{-1} cm^{-1} y^{-1};
- i_{corr} is the corrosion current density in μA cm^{-2};
- ρ is density in g cm^{-3};
- EW is the equivalent weight, dimensionless (EW was calculated assuming the 4th valence of Ti and ignoring the small quantities of alloying elements).

3. Results and discussion

3.1. Weldments structure

Figure 2 represents the macrostructure of one of the weldments. An abrupt boundary between the base metal (BM - 1) and the heat-affected zone (HAZ - 3) is observed in Figure 2, while the transition from HAZ to fusion zone (FZ - 4) is smooth. FZ is characterized by large, up to 3 mm grains.

An interesting phenomenon is the enlarged and elongated morphology of grains in HAZ observed at low magnification and the absence of the typical HAZ with refined (because of the thermal impact) grains. Such a morphology was reported by Fomin et al. [22] in a T-joint of CP-Ti and Ti-6Al-4V, and they concluded that melting occurred till the base metal and no heat-affected zone formed. As the weldments we have made are butt weldments and as it is visible in Figure 2 the HAZ length is around 5 mm, we cannot assume melting occurred so far from the thermal impact in our experiment.

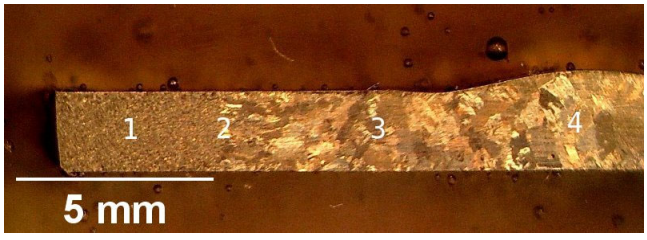

Fig. 2. Macrostructure of a CP-Ti Grade 1 weldment: 1 – base metal (BM); 2 – base metal/heat affected zone boundary; 3 – heat-affected zone (HAZ); 4 – fusion zone (FZ)

Motyka et al. [23] give reasons for this behaviour of titanium and its alloys after thermal impact. In contrast to most polycrystalline metallic materials, titanium does respond differently to grain size changes after heating and cooling. Independently on the cooling conditions, grain growth is observed after heating over the temperature of α→β transformation and next cooling in titanium and titanium alloys. This is connected to some specific Ti properties: 1) its high self-diffusion rates, 2) low modulus of elasticity, and low elastic energy related to the polymorphic transformation, 3) low volume change, 4) low stresses during the polymorphic transformation, and 5) high heat of transformation. These are factors impeding new phase nuclei formation but favouring grain growth. As the weldment macrostructure demonstrates in Figure 2, the grain growth occurred preferentially in the direction of the heat flow, i. e parallel to the welded sheet surface. Thus, the observed here morphology of the weldment's HAZ is attributed to the specific titanium nature and the direction of the heat flow during welding.

Figure 3a represents the microstructure of the base metal in as-recieved condition. The iron content in CP-Ti Grade 1 exceeds the maximal solubility of Fe in α-Ti, and according to the equilibrium Ti-Fe phase diagram [24] CP-Ti Grade 1 is an alloy with an equilibrium structure consisting of α(Ti), FeTi precipitates and [α(Ti) + FeTi] eutectoid.

Nevertheless, the microstructure in Figure 3a does not show any eutectoid. As stated in the specialized literature [25,26], the eutectoid reaction in the Ti-Fe system goes at so low rate that in practice it does not occur even when furnace cooling is applied for hundreds of hours, and some β(Ti)-phase remains at room temperature. Therefore, α-titanium alloys, such as CP-Ti Grade 1, can be regarded as alloyed with β-isomorphous (not β-eutectoid) alloying elements [26]. It was reported [22,25, 27-31] that the microstructure of CP-Ti in as-received condition consisted of α(Ti) and intergranular β(Ti). Optical microscopy of the studied here CP-Ti Grade 1 in as-received condition, as it is visible in Figure 3a, reveals that the BM consists of equiaxed α(Ti)-grains with dimensions between 7 and 80 μm and hardly any highly dispersed β(Ti)-grains. Such an equiaxed grains microstructure of CP-Ti is characteristic for the alloys after recrystallization annealing.

In Figure 3b, the microstructure of the BM/HAZ boundary is represented. A distinct and abrupt change in the grains morphology is observed at this boundary – a sudden change from small, equiaxed grains to large, elongated grains is visible. As small grains are still observed in HAZ, we can conclude the temperature at BM/HAZ boundary was below β-transus and these small grains are untransformed α.

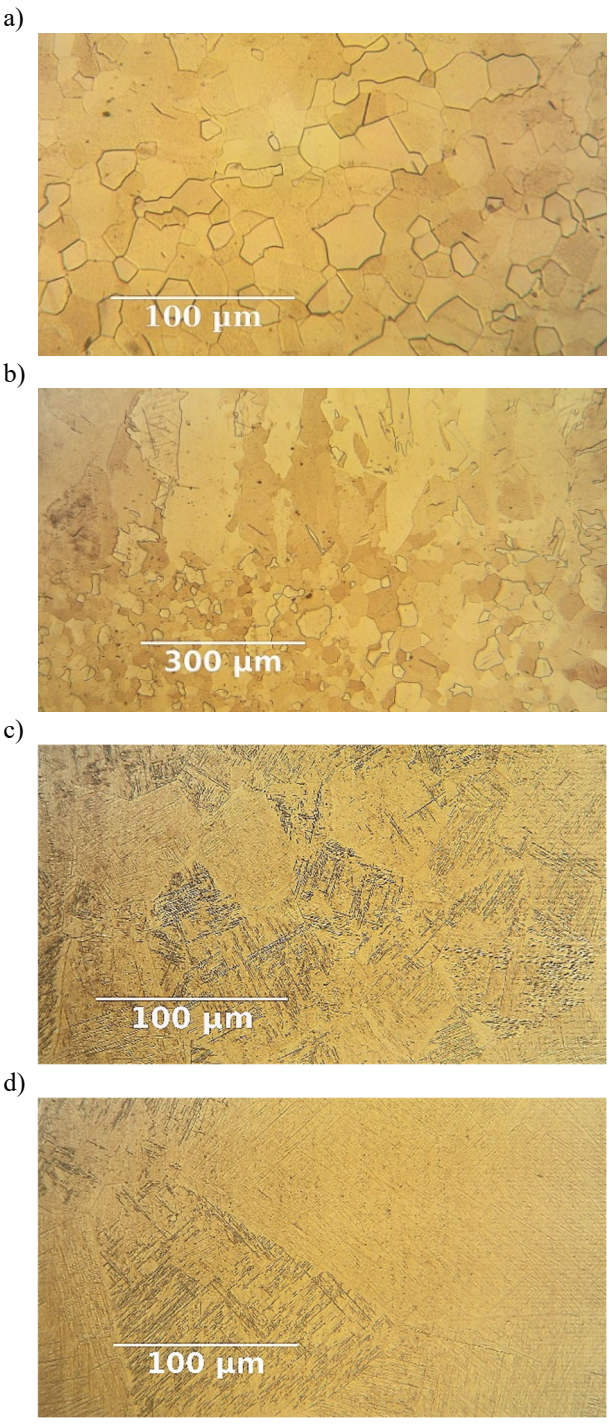

Fig. 3. Microstructure of: a) base metal; b) base metal/heat-affected zone boundary; d) heat-affected zone; e) fusion zone

In Figure 3c, the microstructure of the HAZ can be seen, and in Figure 3d – the microstructure of the fusion zone is visible. Both microphotographs reveal that the visible at the

macrosection in Figure 2 large grains are prior β(Ti)-grains. As it can be seen in Figures 3c and 3d, inside the prior β(Ti)-grains, colonies of long acicular α(Ti)-grains formed; these colonies have different orientations and were differently revealed by the etchant. The grain size of the prior β(Ti)-grains increases from 40-95 μm at HAZ to more than 200 μm at FZ (in Figure 3d only parts of prior β(Ti)-grains are visible).

a)

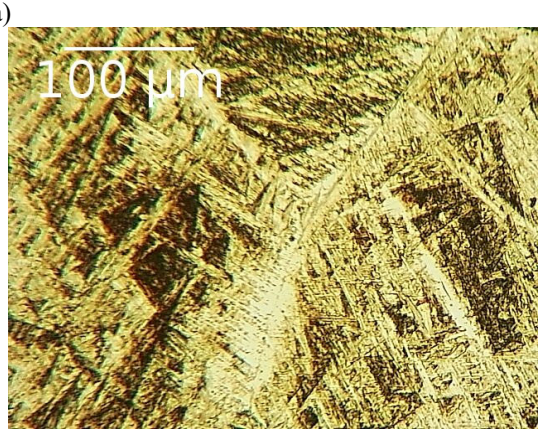

b)

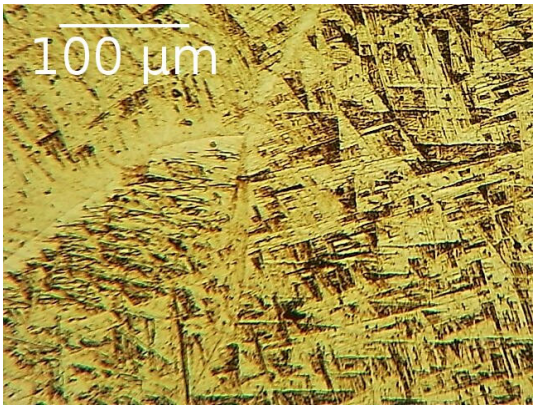

Fig. 4. Microstructure of the electrochemically tested surfaces: a) specimen S1, welded at mode 1; b) specimen 4, welded at mode 4

The microstructure of the electrochemically tested surfaces is presented in Figure 4. These surfaces were obtained after tensile testing of the weldments and represent the position where the fracture occurred, namely, HAZ. The higher magnification allows us to see that the observed at lower magnification acicular α(Ti)-grains represent Widmanstätten microstructure. Some allotriomorphic α(Ti)-phase is observed along the prior β(Ti)-grains boundaries. Similar Widmanstätten microstructure was observed in [32].

3.2. Corrosion behaviour of welded Grade 1

The change in the open circuit potential (OCP) of the studied specimens is shown in Figure 5. Different behaviour of the CP-Ti in as-received condition and after welding is clearly visible. While the open circuit potential of the untreated CP-Ti shows an increase with time, the welded specimens demonstrate a decrease in the OCP. This is indicative of the properties of the passive layers formed on CP-Ti in as-received condition and on the welded specimens. The decrease in OCP for the welded specimens suggests unstable passive layers. The values of the steady-state potential E_{ss} of the samples can be viewed in Table 3 – the difference between E_{ss} of the untreated CP-Ti and HAZ of the welded CP-Ti is more than 120 mV.

After reaching E_{ss} the specimens were polarised starting from -450 mV (NHE) and ending at +1400 mV (NHE). Figure 6 shows the resulting potentiodynamic curves, and Table 3 summarises the electrochemical characteristics of the specimens found from the potentiodynamic curves.

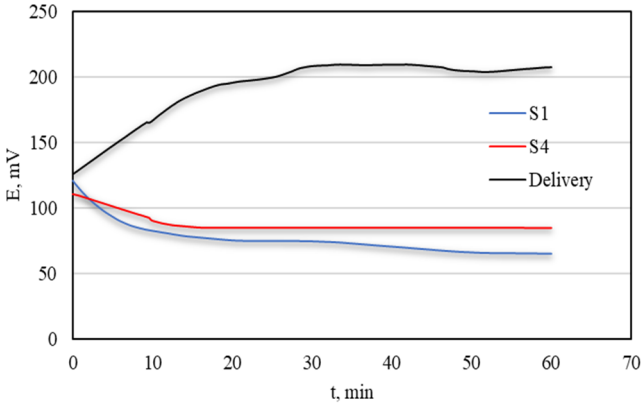

Fig. 5. Open circuit potentials change with time

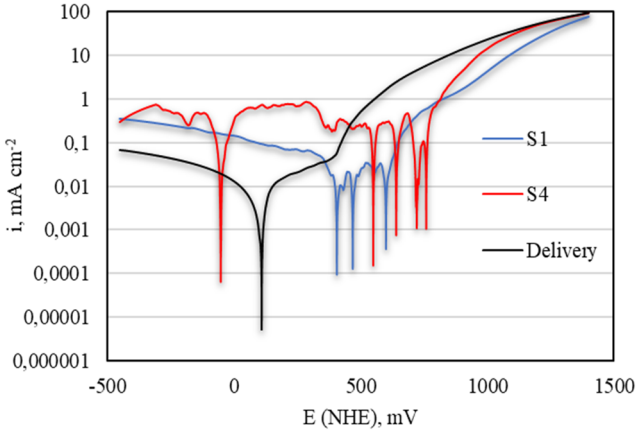

Fig. 6. Potentiodynamic curves of the specimens

Table 3.
Electrochemical characteristics of the specimens

No	Specimen	E_{ss} (NHE), mV	E_{corr} (NHE), mV	E_{pit} (NHE), mV	i_{corr}, mA cm^{-2}	CR, mm y^{-1}
1	As-recieved	+207	+106	+400	0.0011	0.0093
2	S1	+65	+409	+600	0.0072	0.0625
3	S4	+85	-50	+760	0.0403	0.3496

It is visible that the initial cathodic polarisation led to changes in the passive layers shifting the corrosion potentials E_{corr} away from the steady-state potential.

The potentiodynamic curve of the specimen in as-received condition shows anodic dissolution with a low rate, similar to a passive behaviour, in the potential range between the corrosion potential and the breakdown potential (pitting potential E_{pit}) of +400 mV. The potentiodynamic curves of the welded specimens demonstrate an interesting feature, namely, multiple cathodic loops with multiple corrosion potentials. Corrosion potentials listed in Table 3 are the lowest potentials where the transition from cathodic to anodic current happened for the first time; next potentials where cathodic and anodic reactions had the same rate are not listed in this table. Cathodic loops are described in [8,33,34]. These loops result from a cathodic reaction that has a higher rate than the anodic reaction. The higher rate of the cathodic reaction on the surface of the welded specimens is visible already at the cathodic parts of the curves – these parts demonstrate a cathodic current density an order of magnitude higher for the welded specimens compared to the untreated CP-Ti. The multiple cathodic loops indicate unstable passivity leading to pits nucleation and next pits passivation. Figure 7 represents a pit with a diameter of 190 µm on the surface of specimen S4 after the electrochemical testing. Similar pits were observed on all electrochemically tested surfaces. Thus, the abrupt increase in the anodic current density pictures the breakdown (pitting) potential: +600 mV for the specimen, welded at mode 1, and +760 mV for the specimen welded at mode 4.

From all potentials at which anodic and cathodic current densities equal, the lowermost and the uppermost are stable, and the metal spontaneously passes to either of them [33]. This behaviour is not desired from an engineering point as it is unknown what state the metal will become to.

Corrosion current densities i_{corr} were determined at the corrosion potentials listed in Table 3, and then corrosion rates CR were calculated, assuming titanium exchanges four electrons during its corrosion. As it is visible in Table 3, the corrosion rate (CR) of the heat-affected zone of specimen S1 is one order of magnitude higher than the corrosion rate of the untreated CP-Ti, and CR of specimen S4 is even two orders higher. Thus, we can conclude that the welding modes used in our experiment worsened the corrosion resistance of CP-Ti Grade 1. According to the scale of the corrosion resistance of metals [20], CP-Ti Grade 1 is with lower corrosion resistance in 1 M KBr after welding with an elliptical cathode (mode 4) and resistant after welding with a round cathode (mode 1).

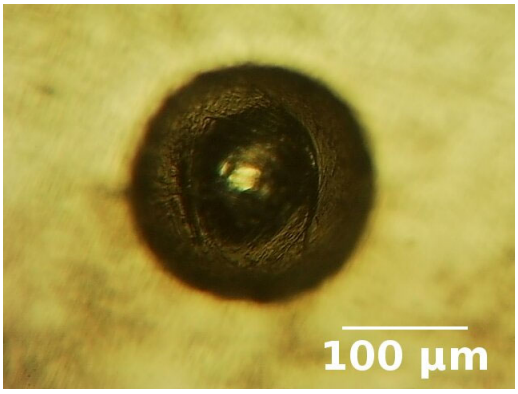

Fig. 7. A pit on the electrochemically tested surface of specimen S4

This strange behaviour of the welded specimens is a repercussion of the coarse Widmanstätten microstructure formed at HAZ during welding. As the resistance of titanium and its alloys to aggressive environments is governed by the passive layer stability, the electrochemical behaviour of the welded specimens suggests that less perfect passive layers formed on the surface of HAZ. A negative impact of Widmanstätten structure on the corrosion resistance of CP-Ti was reported in [35] too.

It is known that the breakdown of the passive layer on titanium occurs at areas where the layer has some defects leading to change in its electrical properties, thus allowing Br^- oxidation to occur and next chemisorption of bromine ions leading to passive layer dissolution [36,37]. In our experiments, these processes occurred at different potentials than the reported in the literature [36,37].

The formation of an imperfect passive layer after welding could be avoided using heat treatment to restore the initial equiaxed microstructure, and our future work has to focus on this.

4. Conclusions

1. Welding with hollow cathode arc discharge in vacuum of CP-Ti Grade 1 leads to the formation of a coarse Widmanstätten microstructure at the heat-affected zone.
2. The Widmanstätten microstructure at the heat-affected zone favours the formation of passive layers with worsened protective properties, thus increasing corrosion rate by up to two orders of magnitude in 1M KBr water solution.
3. The heat-affected zones of the weldments demonstrate unstable corrosion potential in 1M KBr water solution during potentiodynamic polarization.
4. Future experiments including heat treatment for improvement of the passive layers protective properties after welding with hollow cathode arc discharge in vacuum are needed.

References

[1] J. Palán, L. Maleček, J. Hodek, M. Zemko, J. Dzugan, Possibilities of biocompatible material production using conform SPD technology, Archives of Materials Science and Engineering 88/1 (2017) 5-11. DOI: https://doi.org/10.5604/01.3001.0010.7746

[2] J. Klimas, A. Łukaszewicz, M. Szota, K. Laskowski, Work on the modification of the structure and properties of Ti6Al4V titanium alloy for biomedical applications, Archives of Materials Science and Engineering 78/1 (2016) 10-16. DOI: https://doi.org/10.5604/18972764.1226308

[3] L.A. Dobrzański, A. Dobrzańska-Danikiewicz, A. Achtelik-Franczak, The structure and properties of aluminium alloys matrix composite materials with reinforcement made of titanium skeletons, Archives of Materials Science and Engineering 80/1 (2016) 16-30. DOI: https://doi.org/10.5604/18972764.1229614

[4] H. Nishikawa, K. Yoshida, T. Ohji, Y. Suita, K. Masubuchi, Characteristics of hollow cathode arc as welding heat source: arc characteristics and melting properties, Science and Technology of Welding and Joining 7/5 (2002) 280-285. DOI: https://doi.org/10.1179/136217102225004310

[5] T. Ohji, Characteristics of hollow cathode arc as welding heat source. Study on welding in space, Welding International 20/5(2006) 355-360. DOI: https://doi.org/10.1533/wint.2006.3595

[6] Y. Oshida, Oxidation and Oxides, in: Bioscience and Bioengineering of Titanium Materials, Elsevier, 2007, 79-103. DOI: https://doi.org/10.1016/B978-008045142-8/50004-9

[7] P.A. Schweitzer, Fundamentals of Metallic Corrosion: Atmospheric and Media Corrosion of Metals. Corrosion Engineering Handbook, Second Edition, CRC Press/Taylor & Francis Group, 2007.

[8] M.G. Fontana, Corrosion Engineering, McGraw-Hill, New York, 1986.

[9] T.R. Beck, Pitting of Titanium: I. Titanium-Foil Experiments, Journal of The Electrochemical Society 120/10 (1973) 1310-1316. DOI: https://doi.org/10.1149/1.2403253

[10] T.R. Beck, Pitting of Titanium: II. One-Dimensional Pit Experiments, Journal of The Electrochemical Society 120/10 (1973) 1317-1324. DOI: https://doi.org/10.1149/1.2403254

[11] L.F. Garfias-Mesias, M. Alodan, P.I. James, W.H. Smyri, Determination of precursor sites for pitting corrosion of polycrystalline titanium by using different techniques, Journal of The Electrochemical Society 145/6 (1998) 2005-2010. DOI: https://doi.org/10.1149/1.1838590

[12] S.B. Basame, H.S. White, Pitting corrosion of titanium the relationship between pitting potential and competitive anion adsorption at the oxide film/electrolyte interface, Journal of The Electrochemical Society 147/4 (2000) 1376-1381. DOI: https://doi.org/10.1149/1.1393364

[13] I. Dugdale, J.B.Cotton, The anodic polarization of titanium in halide solutions, Corrosion Science 4/1-4 (1964) 397-411. DOI: https://doi.org/10.1016/0010-938X(64)90041-1

[14] T.R. Beck, Stress Corrosion Cracking of Titanium Alloys: I. Ti:8-1-1 Alloy in Aqueous Solutions, Journal of The Electrochemical Society 114/6 (1967) 551-556. DOI: https://doi.org/10.1149/1.2426647

[15] T. Shibata, Y.-C. Zhu, The effect of film formation conditions on the structure and composition of anodic oxide films on titanium, Corrosion Science 37/2 (1995) 253-270. DOI: https://doi.org/10.1016/0010-938X(94)00133-Q

[16] N. Ferdinandov, D. Gospodinov, M. Ilieva, R. Radev, Structure and Pitting Corrosion of Ti-6Al-4V Alloy and Ti-6Al-4V Welds, Proceedings of the 7th International Conference on Advanced Materials and Systems "ICAMS 2018", Bucarest, 2018, 325-330. DOI: https://doi.org/10.24264/icams-2018.VI.7

[17] D.D. Gospodinov, N.V. Ferdinandov, M.D. Ilieva, R.H. Radev, S.P. Dimitrov, Welding of Grade 1 Titnium by hollow cathode arc discharge in vacuum, International Scientific Journal "Machines. Technologies.Materials" 12/5 (2018) 216-218.

[18] M.D. Abramoff, P.J. Magalhaes, S.J. Ram, Image Processing with ImageJ, Biophotonics International 11/7 (2004) 36-42.

[19] J. Hrbac, V. Halouzka, L. Trnkova, J. Vacek, eL-Chem viewer: A freeware package for the analysis of electroanalytical data and their post-acquisition processing, Sensors 14/8 (2014) 13943-13954. DOI: https://doi.org/10.3390/s140813943
[20] J. Klimas, A. Łukaszewicz, M. Szota, K. Szota, Characteristics of titanium Grade 2 and evaluation of corrosion resistance, Archives of Materials Science and Engineering 77/2 (2016) 65-71. DOI: https://doi.org/10.5604/18972764.1225596
[21] A. Łukaszewicz, M. Szota, Influence of production method on selected properties of VT 22 titanium alloy, Archives of Materials Science and Engineering 87/1 (2017) 27-32. DOI: https://doi.org/10.5604/01.3001.0010.5968
[22] F. Fomin, M. Froend, V. Ventzke, P. Alvarez, S. Bauer, N. Kahaev, Metallurgical aspects of joining comercially pure titanium to Ti-6Al-4V alloy in a T-joint configuration by laser beam welding, The International Journal of Advanced Manufacturing Technology 97 (2018) 2019-2031. DOI: https://doi.org/10.1007/s00170-018-1968-z
[23] M. Motyka, K.Kubiak, J. Sieniawski, W. Ziaja, Phase Transformations and Characterization of α + β Titanium Alloys, in: S. Hashmi, G.F. Batalha, C.J. Van Tyne, B. Yilbas (eds.), Comprehensive Materials Processing, Vol. 2, Elsevier, 2014, 7-36. DOI: https://doi.org/10.1016/B978-0-08-096532-1.00202-8
[24] J.L. Murray, The Fe−Ti (Iron-Titanium) system, Bulletin of Alloy Phase Diagrams 2 (1981) 320-334. DOI: https://doi.org/10.1007/BF02868286
[25] G. Lütjering, J.C. Williams, Commercially Pure (CP) Titanium and Alpha Alloys. In: Titanium. Engineering Materials and Processes. Springer, Berlin, Heidelberg, 2003, 175-201. DOI: https://doi.org/10.1007/978-3-540-73036-1_4
[26] I. Polmear, D. StJohn, J.-F. Nie, M. Qian, Light Alloys 5th Edition, Metallurgy of the Light Metals, Butterworth-Heinemann, 2017.
[27] Z.-B. Wang, H.-X. Hu, C.-B. Liu, H.-N. Chen, Y.-G. Zheng, Corrosion Behaviors of Pure Titanium and Its Weldment in Simulated Desulfurized Flue Gas Condensates in Thermal Power Plant Chimney, Acta Metallurgica Sinica (English Letters) 28/4 (2015) 477-486. DOI: https://doi.org/10.1007/s40195-015-0222-z
[28] M. Froend, F. Fomin, S. Riekehr, P. Alvarez, F. Zubiri, S. Bauer, B. Klusemann, N. Kashaev, Fiber laser welding of dissimilar titanium (Ti-6Al-4V/cp-Ti) T-joints and their laser forming process for aircraft application, Optics and Laser Technology 96 (2017) 123-131. DOI: https://doi.org/10.1016/j.optlastec.2017.05.017
[29] P. Yadav, K. Saxena, Effect of heat-treatment on microstructure and mechanical properties of Ti alloys: An overview, Materials Today: Proceedings 26/2 (2020) 2546-2557. DOI: https://doi.org/10.1016/j.matpr.2020.02.541
[30] T. Pasang, Y. Tao, M. Azizi, O. Kamiya, M. Mizutani, W. Misiolek, Welding of titanium alloys, MATEC Web of Conferences 123 (2017) 00001. DOI: https://doi.org/10.1051/matecconf/201712300001
[31] A. Abdollahi, A.S. Ahnaf Huda, A.S. Kabir, Microstructural Characterization and Mechanical Properties of Fiber Laser Welded CP-Ti and Ti-6Al-4V Similar and Dissimilar Joints, Metals 10/6 (2020) 747. DOI: https://doi.org/10.3390/met10060747
[32] J.W. Elmer, J. Wong, T. Ressler, Spatially resolved X-ray diffraction phase mapping and α → β → α transformation kinetics in the heat-affected zone of commercially pure titanium arc welds, Metallurgical and Materials Transactions A 29 (1998) 2761-2773. DOI: https://doi.org/10.1007/s11661-998-0317-5
[33] R.G. Kelly, J.R. Scully, D. Shoesmith, R.G. Buchheit, Electrochemical Techniques in Corrosion Science and Engineering, First Edition, CRC Press, 2002.
[34] E. Blasco-Tamarit, A. Igual-Muñoz, J. García Antón, D. García-García, Corrosion behaviour and galvanic coupling of titanium and welded titanium in LiBr solutions, Corrosion Science 49/3 (2007) 1000-1026. DOI: https://doi.org/10.1016/j.corsci.2006.07.007
[35] A. Guillard,Q. Zhou, Effect of Microstructures on Corrosion Properties of CP-Ti for Medical Applications,Proceedings of the 3rd International Conference on Applied Mechanics and Mechanical Automation "AMMA 2017", Phuket, 2017, 310-316.
[36] N. Casillas, S. Charlebois, W.H. Smyrl, H.S. White, Pitting Corrosion of Titanium, Journal of The Electrochemical Society 14/3 (1994) 636-642. DOI: https://doi.org/10.1149/1.2054783
[37] D. Prando, A. Brenna, M.V. Diamanti, S. Beretta, F. Bolzoni, M. Ormellese, M.P. Pedeferri, Corrosion of Titanium: Part 1: Aggressive Environments and Main Forms of Degradation, Journal of Applied Biomaterials and Functional Materials 15/4 (2017) 291-302. DOI: https://doi.org/10.5301/jabfm.5000387